

Event-by-event viscous hydrodynamics for Cu-Au collisions at $\sqrt{s_{NN}} = 200\text{GeV}$

Piotr Bożek

*The H. Niewodniczański Institute of Nuclear Physics, PL-31342 Kraków, Poland
Institute of Physics, Rzeszów University, PL-35959 Rzeszów, Poland*

Abstract

Event-by-event hydrodynamics is applied to Cu-Au collisions at $\sqrt{s_{NN}} = 200\text{GeV}$. Predictions for charged particle distributions in pseudorapidity, transverse momentum spectra, femtoscropy radii are given. The triangular and elliptic flow coefficients are calculated. The directed flow at central rapidity in the reaction plane in asymmetric collisions is nonzero, fluctuations of the initial profile lead to a further increase of the directed flow when measured in the event plane.

Keywords:

heavy-ion collisions, relativistic hydrodynamics, event-by-event fluctuations, collective flow

The emission of particles with soft momenta in relativistic heavy-ion collisions can be described in a satisfactory way within the relativistic hydrodynamic model [1, 2]. The harmonic flow coefficients are found to be sensitive to the viscosity of the expanding fluid [3–7]. Fluctuations determine the asymmetry of the initial distribution in the transverse plane [8, 9] and event-by-event hydrodynamics simulations are needed to investigate their effect on final spectra [10–15]. Typically collisions of symmetric nuclei are studied experimentally, the most important parameters varied in these analyses are the center of mass energy, the size of the system and the centrality of the collision.

An additional insight into the mechanism of particle production in relativistic heavy-ion collisions can be gained from interactions of two different nuclei, e.g. Cu-Au collisions at $\sqrt{s_{NN}} = 200\text{GeV}$. The study of the multiplicity distribution and correlations in the longitudinal direction in asymmetric collisions gives additional constraints on the mechanism of the energy deposition in the early stage of the reaction [16–20], in particular models assuming approximate boost-invariance of the initial state must be revised. The directed flow [21–24] in asymmetric collisions is partly generated by a new mechanism, as discussed later in this Letter. The measurement of differences between the directed flow of proton and antiprotons could give informations on the different rate of baryon stopping on the Cu and Au side of the fireball which could be compared to model predictions [25–27]. The reaction plane correlations in the fireball [28, 29] are modified in asymmetric collisions, with stronger correlations between odd and even order event planes. As the size and the energy density in the fireball are sufficient to allow for a substantial phase of collective expansion, we apply the event-by-event

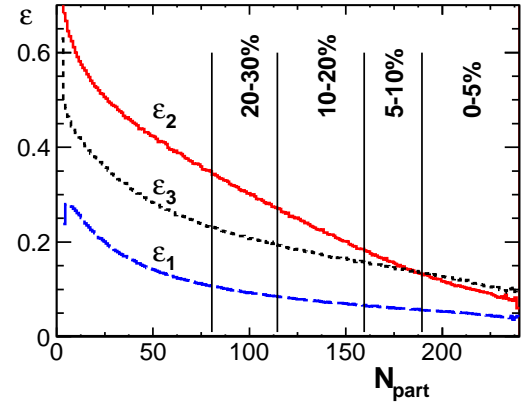


Figure 1: The eccentricity ϵ_2 (solid line), triangularity ϵ_3 (dotted line) and the dipole asymmetry ϵ_1 (dashed line) of the initial fireball as function of the number of participant nucleons in Cu-Au collisions from the Glauber Monte Carlo model [30]. The vertical lines separate different centrality classes.

viscous hydrodynamic model to obtain predictions for basic observables for particles of soft momenta produced in asymmetric Cu-Au interactions.

The second order viscous hydrodynamic equations are solved in 3 + 1-dimensions [13, 31]. We use two values for the shear viscosity coefficient $\eta/s = 0.08$ or 0.16 (unless stated otherwise the default value is 0.08), the bulk viscosity is $\zeta/s = 0.04$ in the hadronic phase. At freeze-out particle emission is performed using a Monte Carlo procedure [32], with a freeze-out temperature of 150MeV . This freeze-out temperature gives a satisfactory description of particle spectra in Au-Au collisions [12]. The hydrodynamic expansion is followed in each event with random

Email address: piotr.bozek@ifj.edu.pl (Piotr Bożek)

initial density. The initial density is generated from the Glauber Monte Carlo model [30] with a Gaussian wounding profile for nucleon-nucleon collisions [33]. The entropy density in the transverse plane x - y and space-time rapidity η_{\parallel} is given as a sum over the participant nucleons

$$s(x, y, \eta_{\parallel}) = d \sum_i f_{\pm}(\eta_{\parallel}) g_i(x, y) [(1 - \alpha) + N_i^{coll} \alpha]$$

weighted with Gaussians $g_i(x, y)$ of width 0.4fm centered at the positions of the participant nucleons i , a term from binary collisions with $\alpha = 0.125$ is included, N_i^{coll} is the number of collisions of the participant nucleon i . The form of the longitudinal profile f_{\pm} and the factor $d = 2.5$ GeV are taken the same as for Au-Au collisions at 200GeV [12]. In Fig. 1 are shown the initial eccentricity ϵ_2 , triangularity ϵ_3 and dipole asymmetry ϵ_1 of the fireball as function of the number of participants, averaged over the initial density with weights r^2 , r^3 and r^3 respectively. In the following we present results for two centrality classes 0-5% and 20-30% defined by the number of participants $190 \leq N_{part}$ and $81 \leq N_{part} \leq 114$ respectively. For each centrality class considered we generate 100 hydrodynamic events, and for each hydrodynamically generated freeze-out configuration 1000-1500 statistical emission events. The relative statistical error on v_2 and v_3 from sampling the initial eccentricity and triangularity distributions with 100 events is 4 – 5%.

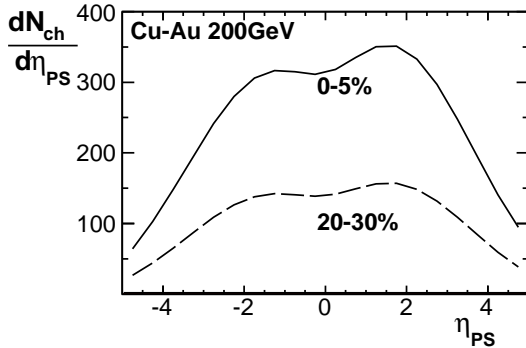


Figure 2: Distribution of charged particles in pseudorapidity for 0-5% (solid line) and 20-30% (dashed line) centrality classes. The Au momentum is directed towards positive rapidity.

The distribution of charged particles in pseudorapidity $dN_{ch}/d\eta_{PS}$ is asymmetric (Fig. 2). It reflects the asymmetry of the initial entropy density (Eq. 1) [19, 34]. The number of participant nucleons is larger in the Au nucleus, with the asymmetry increasing for central collisions. Using the initial condition extrapolated from Au-Au interactions at the same energy, the predicted multiplicities at central rapidity are $dN_{ch}/d\eta_{PS} = 320$ and 140 in 0-5% and 20-30% centrality classes respectively.

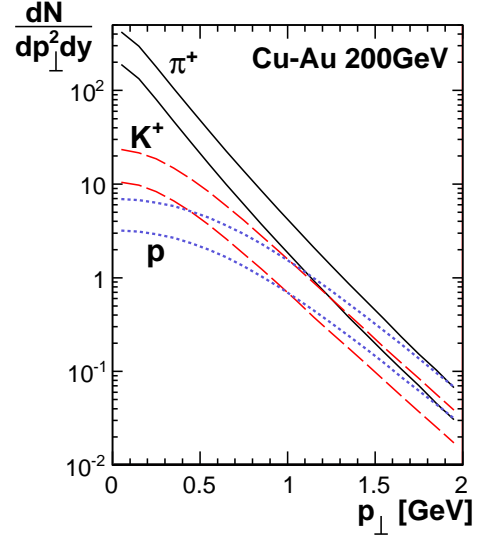


Figure 3: Transverse momentum spectra of π^+ (solid lines), K^+ (dashed lines) and protons (dotted lines) for 0-5% and 20-30% centrality classes (upper and lower curves respectively).

The transverse momentum spectra of π^+ , K^+ and protons shown in Fig. 3 are softer than in Au-Au collisions. The predicted average transverse momenta of pions, kaons and protons in central collisions are 405, 587 and 775 MeV respectively. To obtain correct particle ratios nonzero chemical potentials are introduced at freeze-out, although the equation of state used to calculate the dynamics of the system is at zero baryon density. The equation of state is moderately changing with μ at small baryon densities [36], and the equation of state at zero baryon density can be used for central rapidities in collisions at 200GeV. The energy in the Cooper-Frye formula at freeze-out is conserved to the order μ^2/T^2 . The baryon chemical potential $\mu_B = 22$ MeV at the freeze-out temperature 150 MeV assures the same ratio \bar{p}/p as measured for Au-Au interactions [35].

The elliptic and triangular flow coefficients as function of p_{\perp} are presented in Fig. 4. The differential flow coefficients are calculated using the two-particle cumulant method [37]. The elliptic flow coefficient for semi-central events is significantly larger than in central events. It reflects the larger value of the initial eccentricity in the 20-30% centrality class (Fig. 1). The triangular flow is similar in the two centrality classes studied. With increasing value of shear viscosity the elliptic and triangular asymmetry coefficients are reduced [13, 38]. The influence of shear viscosity is larger in peripheral events and for the triangular flow v_3 [39, 40]. The integrated value of the elliptic flow of charged particles in the p_{\perp} range 150-2000 MeV is 0.022 (0.020) for central and 0.048 (0.043) for peripheral events when $\eta/s = 0.08$ (0.16). The corresponding v_3 coefficients for charged particles are 0.013 (0.011) and 0.016 (0.012).

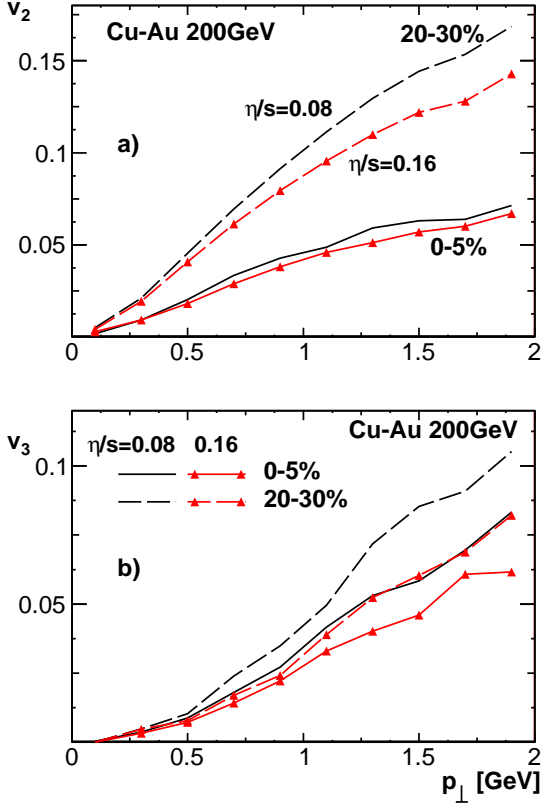


Figure 4: Elliptic (panel a) and triangular (panel b) flow coefficients of charged particles as function of transverse momentum for centralities 0-5% (solid lines) and 20-30% (dashed lines). The results of the calculation with $\eta/s = 0.08$ are presented with lines and for $\eta/s = 0.16$ using lines with triangles.

In collisions of symmetric nuclei at ultrarelativistic energies the directed flow exhibits a component odd in pseudorapidity [21, 22, 41, 42]. At central rapidities nonzero directed flow occurs due to event-by-event fluctuations of the density profile [11, 43–45]. In the fireball created in the collision of two asymmetric nuclei such as Cu-Au collisions the profile is asymmetric in the reaction plane also on average. When defining the reaction plane always with the Au nucleus in the $x > 0$ half plane a nonzero component of the directed flow with respect to the reaction plane appears.

In Fig. 5 is shown the p_T integrated directed flow coefficient v_1 of charged particles with respect to the reaction plane as function of pseudorapidity for centrality 20-30%. At central rapidities the directed flow is negative, more particles flow in the direction of the Cu half plane. Besides the nonzero component even in η_{PS} a smaller odd component of v_1 is visible in Fig. 5. In the hydrodynamic model the odd component of the directed flow is generated from the expansion of the fireball tilted away from the collision axis [21, 22]. The odd component of the directed flow is significantly reduced when viscosity increases, this effect comes from the reduction of the longitudinal pressure in the early phase of the collisions for higher viscosity

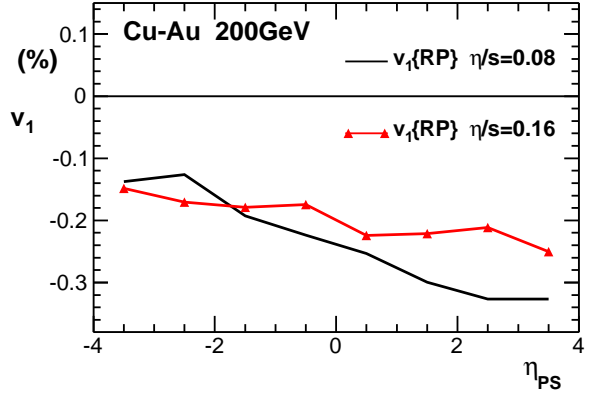


Figure 5: Directed flow of charged particles as function of pseudorapidity with respect to the reaction plane. The results of the calculation with $\eta/s = 0.08$ are presented using a solid line and for $\eta/s = 0.16$ using a solid line with triangles.

[46].

The even component of the directed flow as function of transverse momentum in the reaction plane

$$v_1(p_\perp)\{RP\} = \langle \cos(\phi_i - \Psi_{RP}) \rangle \quad (2)$$

is estimated as the average for charged particles with $|\eta_{PS}| < 1$. The direction of the reaction plane Ψ_{RP} is chosen in the direction of the Au nucleus. Defining the reaction plane using all the nucleons in the Au and Cu nuclei or only the spectator nucleons in the two nuclei in each event gives indistinguishable results. The directed flow $v_1(p_\perp)$ is negative for small momenta and changes sign for $p_\perp \simeq 850\text{MeV}$ (Fig. 6). The component of the directed flow odd in pseudorapidity

$$v_1(p_\perp)\{RP\}(odd) = \langle \text{sgn}(\eta_{PS}) \cos(\phi_i - \Psi_{RP}) \rangle \quad (3)$$

is much smaller than the even one (we take charged particles with $|\eta_{PS}| < 2$).

Fluctuations of the fireball density in each event change the orientation and the magnitude of the directed flow in each event [43]. We follow the procedure of Refs. [11, 47], where the Q vector of the event plane is defined with a weight reducing the contribution of momentum conservation to the directed flow

$$Q e^{i\Psi_1} = \langle w_i e^{i\phi_i} \rangle \quad (4)$$

with $w_i = p_\perp - \langle p_\perp^2 \rangle / \langle p_\perp \rangle$. The Q weighted value of the directed flow coefficient is

$$v_1(p_\perp)\{EP\} = \frac{\langle Q \cos(\phi_i - \Psi_1) \rangle}{\sqrt{\langle Q^2 \rangle}} \quad (5)$$

The directed flow coefficient $v_1(p_\perp)$ with respect to the event plane has the same form as the even component defined in the reaction plane, but with a slightly larger magnitude (solid line in Fig. 6). This means that fluctuations increase the directed flow at central rapidity. The

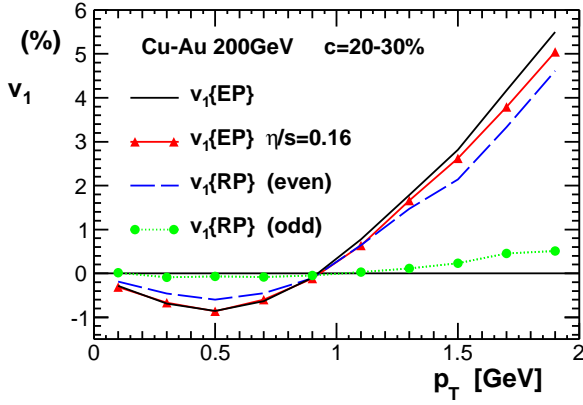


Figure 6: Directed flow of charged particles as function of transverse momentum with respect to the reaction plane (dashed line) and the event plane (solid lines) for $|\eta_{PS}| < 1$, the dots represent the directed flow with respect to the reaction plane odd in pseudorapidity for $|\eta_{PS}| < 2$. The results of the calculation of $v_1\{EP\}$ with $\eta/s = 0.16$ are presented using a solid line with triangles.

calculated directed flow in the event plane does not depend strongly on the value of shear viscosity.

The correlation function for same charge pion pairs is calculated using the momenta and positions of pions emitted in each event [32, 48]. From the correlation function in relative momentum of the pair the femtoscopy radii are extracted. In Fig. 7 is shown the dependence of the three radii R_{out} , R_{side} , and R_{long} on the average pion momentum. This dependence is similar as seen in Au-Au collisions, but with smaller values of the radii. In addition, we calculate the femtoscopy radii using one hydrodynamic simulation starting from the average initial condition corresponding to centrality 0-5% (solid lines in Fig 7). The results are very similar as obtained in event by event simulations. It shows that flow fluctuations in the event by event evolution are too small to affect significantly the femtoscopy radii.

We present predictions of the event by event viscous hydrodynamic model for Cu-Au collisions at $\sqrt{s_{NN}} = 200\text{GeV}$. The charged particle multiplicity and femtoscopy radii are smaller than in Au-Au interactions, reflecting the reduced size of the system. The transverse momentum spectra are steeper and the elliptic and triangular flow smaller than for the Au-Au system.

A novel aspect for collisions of asymmetric nuclei is seen in the directed flow. The asymmetry of the fireball density in the reaction plane leads to the formation of a directed flow of charged particles at central rapidities. This contribution appears when the orientation of the pair of Cu and Au nuclei in the reaction plane is determined in each event and is nonzero also in the absence of density fluctuations. Density fluctuations further increase the directed flow at central rapidities when measured in the reaction plane.

Acknowledgment:

Supported by Polish Ministry of Science and Higher Ed-

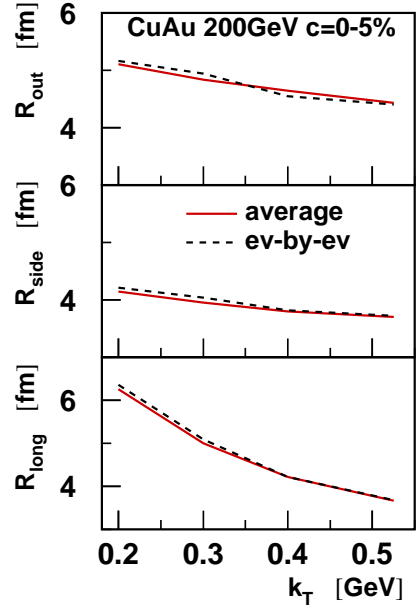


Figure 7: The femtoscopy radii R_{out} , R_{side} , and R_{long} as function of the average transverse momentum of the pion pair. The dashed lines represent the results of the event-by-event hydrodynamics and the solid lines the results obtained in a simulation using one average initial condition.

ucation, grant N N202 263438.

References

- [1] P. F. Kolb, U. W. Heinz, in: R. Hwa, X. N. Wang (Eds.), Quark Gluon Plasma 3, World Scientific, Singapore, 2004, p. 634.
- [2] W. Florkowski, Phenomenology of Ultra-Relativistic Heavy-Ion Collisions, World Scientific Publishing Company, Singapore, 2010.
- [3] P. Romatschke, Int. J. Mod. Phys. E19 (2010) 1.
- [4] K. Dusling, D. Teaney, Phys. Rev. C77 (2008) 034905.
- [5] H. Song, S. A. Bass, U. Heinz, Phys. Rev. C83 (2011) 054912.
- [6] H. Niemi, G. S. Denicol, P. Huovinen, E. Molnar, D. H. Rischke, Phys. Rev. Lett. 106 (2011) 212302.
- [7] P. Bożek, Phys. Rev. C81 (2010) 034909.
- [8] B. Alver, et al., Phys. Rev. C77 (2008) 014906.
- [9] B. Alver, G. Roland, Phys. Rev. C81 (2010) 054905.
- [10] R. Andrade, F. Grassi, Y. Hama, T. Kodama, J. Socolowski, O., Phys. Rev. Lett. 97 (2006) 202302.
- [11] F. G. Gardim, F. Grassi, Y. Hama, M. Luzum, J.-Y. Ollitrault, Phys. Rev. C83 (2011) 064901.
- [12] P. Bożek, W. Broniowski, Phys. Rev. C85 (2012) 044910.
- [13] B. Schenke, S. Jeon, C. Gale, Phys. Rev. Lett. 106 (2011) 042301.
- [14] Z. Qiu, C. Shen, U. Heinz, Phys. Lett. B707 (2012) 151.
- [15] A. Chaudhuri, Phys. Lett. B710 (2012) 339.
- [16] S. Gavin, L. McLerran, G. Moschelli, Phys. Rev. C79 (2009) 051902.
- [17] F. Gelis, T. Lappi, R. Venugopalan, Nucl. Phys. A830 (2009) 591c.
- [18] K. Dusling, T. Epelbaum, F. Gelis, R. Venugopalan, arXiv:1207.5401 [hep-ph] (2012).
- [19] A. Białas, W. Czyż, Acta Phys. Polon. B36 (2005) 905.
- [20] A. Białas, K. Zalewski, Phys. Lett. B698 (2011) 416.
- [21] P. Bożek, I. Wykiel, Phys. Rev. C81 (2010) 054902.

- [22] R. Andrade, A. Reis, F. Grassi, Y. Hama, T. Kodama, et al., Indian J.Phys. 84 (2010) 1657.
- [23] L. P. Csernai, D. Rohrlich, Phys. Lett. B458 (1999) 454.
- [24] R. J. M. Snellings, H. Sorge, S. A. Voloshin, F. Q. Wang, N. Xu, Phys. Rev. Lett. 84 (2000) 2803.
- [25] S. Vance, M. Gyulassy, X. Wang, Phys. Lett. B443 (1998) 45.
- [26] H. Weber, E. Bratkovskaya, H. Stoecker, Phys. Rev. C66 (2002) 054903.
- [27] Y. Mehtar-Tani, G. Wolschin, Phys. Rev. Lett. 102 (2009) 182301.
- [28] P. Bożek, W. Broniowski, J. Moreira, Phys. Rev. C83 (2011) 034911.
- [29] R. S. Bhalerao, M. Luzum, J.-Y. Ollitrault, Phys. Rev. C84 (2011) 054901.
- [30] W. Broniowski, M. Rybczyński, P. Bożek, Comput. Phys. Commun. 180 (2009) 69.
- [31] P. Bożek, Phys. Rev. C85 (2012) 034901.
- [32] M. Chojnacki, A. Kisiel, W. Florkowski, W. Broniowski, Comput. Phys. Commun. 183 (2012) 746.
- [33] M. Rybczynski, W. Broniowski, Phys. Rev. C84 (2011) 064913.
- [34] P. Bożek, Phys. Rev. C85 (2012) 014911.
- [35] I. Bearden, et al., Phys. Rev. Lett. 90 (2003) 102301.
- [36] M. Bluhm, B. Kampfer, R. Schulze, D. Seipt, U. Heinz, Phys. Rev. C76 (2007) 034901.
- [37] N. Borghini, P. M. Dinh, J.-Y. Ollitrault, Phys. Rev. C63 (2001) 054906.
- [38] M. Luzum, P. Romatschke, Phys. Rev. C78 (2008) 034915.
- [39] H. Song, U. W. Heinz, Phys. Rev. C78 (2008) 024902.
- [40] B. H. Alver, C. Gombeaud, M. Luzum, J.-Y. Ollitrault, Phys. Rev. C82 (2010) 034913.
- [41] B. B. Back, et al., Phys. Rev. Lett. 97 (2006) 012301.
- [42] B. I. Abelev, et al., Phys. Rev. Lett. 101 (2008) 252301.
- [43] D. Teaney, L. Yan, Phys. Rev. C83 (2011) 064904.
- [44] G. Aad, et al., Phys.Rev. C86 (2012) 014907.
- [45] I. Selyuzhenkov, J.Phys.G G38 (2011) 124167.
- [46] P. Bożek, I. Wyskiel-Piekarska, Phys. Rev. C83 (2011) 024910.
- [47] M. Luzum, J.-Y. Ollitrault, Phys. Rev. Lett. 106 (2011) 102301.
- [48] A. Kisiel, W. Florkowski, W. Broniowski, J. Pluta, Phys. Rev. C73 (2006) 064902.